

1 **Was Scotland covered by an ice sheet during Marine Isotope Stage 4? Insights from the**
2 **pre-Last Glacial Maximum marine terraces of northwest Scotland**

3 Running Title: Pre-LGM marine terraces of NW Scotland

4 *Alexander R. Simms¹, Regina DeWitt², Sarah L. Bradley³, Emily Huffman¹, Louise Best⁴, Tom*
5 *Bradwell⁵, Jerry Lloyd⁶, and Samuel B. Kachuck⁷*

6 *¹Department of Earth Science, University of California Santa Barbara, 1006 Webb Hall, Santa*
7 *Barbara, CA 93106, USA*

8 *²Department of Physics, East Carolina University, C-109 Howell Science Complex, MS-563,*
9 *Greenville, NC 27858, USA*

10 *³School of Geography and Planning, University of Sheffield, Winter Street, Sheffield S3 7ND,*
11 *UK*

12 *⁴School of Education and Science, University of Gloucestershire, Cheltenham GL20 2RH, UK*

13 *⁵Biological and Environmental Sciences, University of Stirling, Stirling FK9 4LA, UK*

14 *⁶Department of Geography, Durham University, South Road, Durham DH1 3LE, UK*

15 *⁷Climate and Space Sciences and Engineering Department, University of Michigan, 2455*
16 *Hayward Street, Ann Arbor, MI 48109, USA*

17

18

19 **Abstract**

20 Raised shorelines provide important constraints on past sea levels, glacial isostatic
21 adjustment (GIA), and rates and directions of vertical crustal motion. Although most raised
22 shorelines across NW Scotland relate to post-Last Glacial Maximum (LGM) glacial-isostatic
23 rebound, many undated shorelines lie above the marine limit established from isolation basins.
24 Here we present new optically stimulated luminescence (OSL) ages for a raised marine terrace at
25 an elevation of 28 m in Slaggan Bay of NW Scotland. Four OSL ages suggest the feature is pre-
26 LGM, likely Marine Isotope Stage (MIS) 3. Global mean sea levels (GMSL) during MIS 3 are
27 thought to have been ~40-60 m below present across most of the globe. We use a pair of GIA
28 models to determine what ice sheet and sea-level scenarios might provide an explanation for
29 these anomalously high sea levels during MIS 3. Our results suggest that in the absence of
30 tectonic activity, such high MIS 3 shorelines across NW Scotland require a MIS 4 ice sheet in
31 Scotland with post-glacial rebound of the crustal depression following its demise during MIS 3
32 responsible for the elevated shoreline features at that time.

33 **Keywords:** British-Irish Ice Sheet, Interstadial, sea-level change, Interglacial, coastal

34

35 **1. Introduction**

36 Although global mean sea levels (GMSLs) and ice sheet volumes are reasonably well
37 known during the Last Glacial Maximum (LGM) and the Last Interglacial, our understanding of
38 GMSLs and ice sheet volumes during the intervening MIS 3 and MIS 4 are poorly constrained.
39 For example, estimates of MIS 3 GMSLs range from -37 m (Pico et al., 2020) to -60 m (Siddall
40 et al., 2008) relative to present (Gowan et al., 2021). Our understanding of ice volumes during

41 MIS 3 and MIS 4 are even more poorly constrained (Dalton et al., 2022a; Doughty et al., 2021).
42 Recent work has refined our understanding of these ice sheets across North America (e.g. Dalton
43 et al., 2019; 2022b; Pico et al., 2018), South America (e.g. Peltier et al., 2021) and Fennoscandia
44 (Kleman et al., 2021). This recent work has led to many new global ice models to include ice
45 during MIS 4 across much of the Northern Hemisphere including Scotland (e.g. Batchelor et al.,
46 2019; Gowan et al., 2021). However, evidence for a MIS 4 ice sheet in Scotland and the British
47 Isles is fragmentary but growing (Scourse, 2024). With only a handful of ages on pre-LGM
48 bedrock ice-abraded surfaces (e.g. Rolfe et al., 2012; Gibbard et al., 2022; Hughes et al., 2022),
49 moraines, till, or outwash fans (e.g. Duller et al., 1995; Bradwell et al., 2021; Rex et al., 2023),
50 much of that evidence comes from ice rafted debris along the margins of the British Isles (Knutz
51 et al., 2001; Wilson et al., 2002; Scourse et al., 2009; Peck et al., 2007; Toucanne et al., 2009;
52 2023; Hibbart et al., 2010; Fabien et al., 2023) but some is from anomalously elevated relative
53 sea levels (e.g. Dawson et al., 1997; O’Cofaigh et al., 2012; Gallagher et al., 2015).

54 Across NW Scotland, similar to other formerly glaciated margins, higher-than-present
55 relative sea levels (RSL) were experienced immediately following the LGM due to the delayed
56 surface response to the unloading of former ice sheets. As glaciers are effective agents at
57 eroding the landscape, most of these raised shorelines date to post-LGM times. The two
58 regionally mappable raised shorelines across NW Scotland include (i) the Lateglacial shoreline,
59 which formed immediately after the LGM, and (ii) the Post-glacial shoreline, which formed
60 during the mid-Holocene (Smith et al., 2019). However, fragments of older shorelines have been
61 found (e.g. Robinson, 1977; Smith et al., 2019; Dawson et al., 2023). These older shorelines are
62 poorly dated and thus their age and importance in understanding sea-level and ice-sheet changes
63 across Scotland remain unknown. In this study we add to a growing body of evidence on the

64 pre-LGM ice sheets and sea-level constraints of NW Scotland (e.g. Dawson et al., 1997) by
65 reporting the first absolute ages from one of these pre-LGM shorelines in NW Scotland north of
66 the Isle of Skye. At Slaggan Bay, approximately 4 km SW of Greenstone Point, a marine terrace
67 underlain by ~20 m of Quaternary deposits lies ~10 m above the Lateglacial shoreline mapped
68 by Sissons and Dawson (1981) (Fig. 1). We obtained 4 new OSL ages from the topset and
69 foreset deposits associated with this raised marine terrace. In addition, we note the presence of
70 other similar features lying above the generally accepted Lateglacial shoreline across NW
71 Scotland. We review these elevations and compare them with GIA model results to determine
72 what ice sheet and GMSL scenarios might result in higher-than-present pre-LGM sea levels
73 across NW Scotland. Our new results add to a growing, but still fragmentary, understanding of
74 the pre-LGM (pre-MIS 2) ice-sheet and sea-level history of Scotland.

75 **2. Background**

76 *2.1 Ice Sheet and Sea-level History*

77 Ice sheets covered Scotland during the LGM when its ice sheet merged with the
78 Fennoscandian Ice Sheet (Hughes et al., 2016) and extended to the continental shelf edge (Clark
79 et al., 2018). Little is known about the ice sheet extent and thickness prior to the LGM (Scourse,
80 2024), but the region experienced multiple phases of glaciation over the last 1.1 to 2.6 Ma
81 (Thierens et al., 2012; Gibbard et al., 2022). Currently evidence for these previous glaciations is
82 fragmentary (Gemmell et al., 2007; Smith et al., 2019; Gibbard et al., 2022; Scourse, 2024) due
83 in part to the erosive nature of subsequent glaciations (Merritt et al., 2019). Records of ice-rafted
84 debris (IRD) in marine sediment cores in the North Atlantic suggested the presence of marine-
85 terminated glaciers across western Scotland during MIS 4 (Knutz et al., 2001; Wilson et al.,
86 2002; Hibbert et al., 2010; Peck et al., 2007; Scourse et al., 2009; Fabien et al., 2023). Marine

87 cores also provide evidence for enhanced meltwater delivery to the surrounding oceans from the
88 British Isles during early MIS 4 (Toucanne et al., 2023). On land, Bradwell et al. (2021) in NW
89 Scotland and Duller et al. (1995) and Gemmell et al. (2007) in NE Scotland used OSL to date
90 glacial-fluvial outwash deposits that suggest glacial meltwater during MIS 4 (Fig. 1a). Farther
91 south in England and Wales, evidence for MIS 4 glaciation includes cosmogenic ages of glacial
92 landforms (e.g. Rolfe et al., 2012; Gibbard et al., 2022; Hughes et al., 2022) and glacial-fluvial
93 deposits (e.g. Rex et al., 2023) and tills younger than MIS5 but older than the LGM (Bowen,
94 1991; Merritt and Auton, 2000; Finlayson et al., 2010; Scourse, 2024). However, discussion
95 continues as to the absolute age and origin of many of these terrestrial deposits and landforms
96 (Clark et al., 2004; Scourse, 2024).

97 Following retreat of the LGM ice masses, most of Scotland underwent postglacial
98 rebound. The highest magnitudes of uplift were located SE of our study area (e.g. Smith et al.,
99 2006) where raised beaches and isolation basins suggest RSLs as high as 40 m during
100 deglaciation (Shennan et al., 2018; Dawson et al., 2022). Generally, these marine limits decrease
101 north of the Isle of Skye to an elevation of around 20 m in the vicinity of Slaggan Bay (Sissons
102 and Dawson, 1981; Shennan et al., 2018; Simms et al., 2022) along the eastern shores of the
103 Minch (Fig. 1). However, older, presumably higher raised marine deposits have been identified
104 (e.g. Robinson, 1977). In other areas of Scotland (e.g. Dawson et al., 1997) and Ireland (e.g.
105 O’Cofaigh et al., 2012; Gallagher et al., 2015) luminescence ages of these older marine deposits
106 including raised beaches have suggested these postdate the last interglacial but pre-date the
107 LGM. Some previous work has suggested that the elevations of these higher and presumably
108 older marine indicators may be a result of rebound from pre-LGM ice masses (e.g. Sutherland,

109 1981; O' Cofaigh et al., 2012; Scourse, 2024) but to date no studies have explicitly tested these
110 ideas with a GIA model.

111 *2.2 Study areas*

112 Slaggan Bay is a small cove on Greenstone Point Peninsula near the mouth of Loch Ewe,
113 which opens into the Minch – the strait between mainland Scotland and the Outer Hebrides (Fig.
114 1). The whole rugged Greenstone Point headland is underlain by Neoproterozoic sandstones of
115 the Torridon Group. Following the LGM, the headland was likely ice free by 17-16 ka
116 (Bradwell et al., 2021). The post-LGM marine limit is thought to be around 20 m in this region
117 (e.g. Sissons and Dawson, 1981; Shennan et al., 2018; Simms et al., 2022). Stoer Peninsula is
118 another prominent headland about 40 km north of Slaggan Bay (Fig. 1). It too was covered by
119 ice during the LGM and became ice free at about the same time as Slaggan Bay (Bradwell et al.,
120 2021), or slightly earlier. However, the post-LGM marine limit is thought to be much lower
121 here, likely less than 6 m (Hamilton et al., 2015).

122 **3. Methods**

123 *3.1 Field Sampling*

124 All sites were surveyed to Ordnance Datum Newlyn (OD). The marine terraces at
125 Slaggan Bay were surveyed using a Leica 1200 differential GPS. At Stoer Peninsula, the marine
126 terrace was levelled using a Leica Automatic Optical Level in reference to an adjacent fixed
127 Ordnance Survey benchmark (NC00503261). In addition, the sedimentary deposits comprising
128 the marine platforms were observed in scarps cut into both platforms. Sands for OSL dating at
129 Slaggan Bay were sampled under a large opaque black tarpaulin sheet. Dose-rate samples were
130 collected from each distinct layer within a distance of 40 cm above and below the sample.

131 3.2 *Optically Stimulated Luminescence Dating*

132 Quartz separates were prepared by treating 90-212 μm diameter grains with 27% H_2O_2 ,
133 10% HCl , and 48% HF for 40 min, and subsequent density separation with lithium polytungstate
134 solution (densities 2.75 g/cm^3 and 2.62 g/cm^3). After quartz extraction, samples were sieved once
135 more to narrow down the grain size fraction. For each sample the fraction with the most grains
136 was chosen for dating. We used 3mm quartz aliquots, prepared on stainless steel discs using
137 silicone spray. Measurements were conducted using a Risø TL/OSL-DA-20 reader, Risø
138 National Laboratory, with a bialkali PM tube (Thorn EMI 9635QB) and Hoya U-340 filters
139 (290-370 nm). The built-in $^{90}\text{Sr}/^{90}\text{Y}$ beta source gives a dose rate of $\sim 100 \text{ mGy/s}$, and the exact
140 dose rate was calculated for each measurement. Optical stimulation was carried out with blue
141 LEDs (470 nm), delivering 82 mW/cm^2 to the sample. IR stimulation was from an IR LED array
142 at $875\pm 80 \text{ nm}$ with 124 mW/cm^2 power at the sample. The heating rate used was $5 \text{ }^\circ\text{C/s}$.

143 We used a Single-Aliquot Regenerative-dose (SAR) method for determination of the
144 equivalent dose (Wintle and Murray, 2006). Dose recovery and plateau tests resulted in a preheat
145 temperature of 180°C . Dose responses were fitted with a saturating exponential function.
146 Samples generally showed bright signals and good recycling ratios, with negligible IR depletion.
147 Aliquots with recycling ratios between 0.9 and 1.1, and IR depletion $<10\%$ were used for
148 calculating the equivalent dose (Duller, 2003) based on the common age model (Galbraith,
149 1999). All errors are reported as 1 sigma.

150 U, Th, and K concentrations in the samples were measured with high resolution Ge gamma
151 spectrometry with a Reverse Electrode Coaxial Germanium detector from Canberra Industries,
152 Inc. No disequilibria in the uranium decay chain were observed. Water content was calculated as
153 mass of water divided by mass of dry sample. The measured values were used with an

154 uncertainty of 0.01. Dose rate from cosmic rays was determined from the depth of sample below
155 the surface along with its longitude, latitude and altitude, as described by Prescott and Hutton
156 (1994).

157 *3.3 Glacial Isostatic Adjustment (GIA) Modeling*

158 In order to determine what sea-level elevations for NW Scotland are reasonable over the
159 last glacial cycle, we used the GIA model developed by Bradley et al. (2023), which is an
160 outgrowth of several preceding models (e.g. Bradley et al., 2011) to predict past sea levels. To
161 produce the RSL and land level predictions across our study region, we solved the generalized
162 sea-level equation (Kendall et al., 2005, Mitrovica and Milne, 2003), including the impact of
163 rotation and time-dependent shoreline migration combined with a 1D spherically symmetric,
164 self-gravitating Earth model. The GIA model was run at 512 spherical harmonics giving it a
165 resolution of ~ 35 km.

166 We considered two different ice sheet reconstructions combined with their associated
167 earth model. The first, GLAC1D+, is a more traditional reconstruction based on the model of
168 Tarasov et al. (2012) but modified over the British Isles and Europe by Bradley et al. (2023). It
169 was combined with a lithosphere thickness of 71 km, an upper mantle viscosity of 5×10^{20} Pa s,
170 and a lower mantle viscosity of 1×10^{22} Pa s. Within this reconstruction, no ice is found over the
171 British Isles including Scotland during MIS4 and GMSLs during MIS3 are no higher than -53 m
172 below present. As there is no ice across Scotland at MIS4, the RSL and land level will be driven
173 by the other large continental ice sheets across North America and Antarctica. The second is
174 based on the PALEOMIST ice sheet reconstruction of Gowan et al. (2021), which contains
175 significantly more ice in the northern Hemisphere including Scotland during MIS4 and GMSLs
176 during MIS3 reach as high as -27 m at approximately 42 ka (Fig. 4). It was combined with an

177 earth model with a lithosphere thickness of 71 km, an upper mantle viscosity of 5×10^{20} Pa s, and
178 a lower mantle viscosity of 5×10^{22} Pa s. Although this model is the topic of much discussion (e.g.
179 Yokoyama et al., 2021), it nevertheless provides an ice sheet model openly available with a clear
180 MIS4 ice sheet over the northern hemisphere ice centers including Scotland.

181

182 **4. Results**

183 *4.1 Slaggan Bay*

184 A very well-developed marine terrace with a top elevation of 28.3 ± 1.1 m (OD) is found
185 at Slaggan Bay (Fig 2a). The marine terrace extends for nearly 2 km between the southern
186 shores of Slaggan Bay to a few hundred meters north of Gob a' Gheodha (Fig. 1). A similar
187 marine terrace continues to the north but at a lower elevation of around 17.5 m OD. The higher
188 ~28 m marine terrace is composed of a ~20 m thick succession of Quaternary deposits
189 unconformably overlying Torridonian Sandstones (Fig. 2a,b). Although partly obscured by
190 vegetation cover, the Quaternary section is composed of diamicton at the base, overlain by thin
191 to medium bedded coarse, medium, and fine sands with occasional pale grey silt lenses (Fig.
192 2d,e,f). The tan-colored bedded sands are well sorted within each bed and overprinted with
193 pedogenic lamellae. The top of the succession is composed of medium to very thick beds and
194 lenses of dark brown to black gravelly coarse sand or sandy gravels with cobbles up to 20 cm in
195 diameter (Fig. 2d). The bedding planes are wavy and the deposits have weakly developed cross-
196 bedding, ripple cross-lamination, and imbrication. Some of the upper beds are cemented. The
197 whole feature is draped by a 20-30 cm gravelly colluvial cover with isolated peat accumulations.

198 *4.2 Stoer Peninsula*

199 A well-developed paleo-wave-cut platform with a shoreline angle elevation of 25.0 ± 0.25
200 m is found on Stoer Peninsula (Fig. 2c). The platform is cut into a stiff diamicton (Fig. 2g),
201 which is found within at least the upper 1 m of a ~ 13 m section of Quaternary deposits overlying
202 a near horizontal unconformity cut into the underlying Torridonian sandstone. The wave-cut
203 platform may be composed of two distinct levels, but a non-marine origin to the upper platform
204 cannot be ruled out.

205 *4.3 OSL ages*

206 We obtained 4 new OSL ages from the deposits at Slaggan Bay (Tables 1 and 2). Three
207 ages were collected from the lower bedded sands: two from the base of the platform (GA22-12
208 and GA22-13) and one from the middle section of the platform (GA22-15) (Figs. 2a,b;3). The
209 fourth age was obtained from a well-cemented bed at the top of the platform at an elevation of 25
210 m OD within the black gravelly sands (GA22-14; Fig. 2d). One of the samples within the lower
211 bedded sands (GA22-12) returned a minimum age of >109 ka. The majority of aliquots from
212 this sample were saturated and the minimum age was calculated using an equivalent dose of 2
213 D_0 , where D_0 is the characteristic dose of the saturating exponential function. The lowest dose of
214 the few unsaturated aliquots was ~ 250 Gy, representing an age of 90 ka. GA22-13 and GA22-14
215 both returned ages within error of 53.5 ± 5.7 ka and 49.4 ± 3.6 ka, respectively (Fig. 3). The fourth
216 sample, GA22-15, from the bedded sands of the middle platform returned an age of 24.0 ± 1.7 ka
217 (Fig. 3).

218 **5. Discussion**

219 *5.1 Origin, age and preservation of the Slaggan Bay high marine terrace*

220 The Quaternary deposits comprising the 28 m terrace at Slaggan Bay are interpreted to
221 represent a shoreline/delta. The cobbles are well rounded and oblate in shape. The cross-
222 bedding and ripple cross-lamination indicate traction deposition and, in combination with the
223 wavy nature of the bedding, are consistent with wave influence within a beach-like system or
224 beach plain of an outwash delta. The overall shape of the feature is similar to other raised
225 marine shorelines and terraces across Scotland (e.g. Sissons and Dawson, 1981). In addition, its
226 orientation parallel to the modern coast fits that of a marine rather than fluvial origin. We thus
227 interpret the black sandy gravels and gravelly sands at the top of the feature as topsets of the
228 marine shoreline/delta while the bedded sands in the middle and base of the feature are the
229 foresets of the marine shoreline/delta (Fig. 3). The diamictons both at Slaggan Bay and Stoer
230 Peninsula are matrix-supported with an abundance of both well-rounded and angular, striated,
231 clasts of diverse lithologies (Fig. 2f,g). Based on these characteristics, we interpret them to
232 represent tills from a pre-LGM glaciation.

233 Although our 4 new OSL ages are not the same age, they clearly show that the platform is
234 pre-LGM in age (Fig. 3). Two of the ages are within error, GA22-13 and GA22-14 at 53.5 ± 5.7
235 ka and 49.4 ± 3.6 ka, respectively. These two ages were obtained from different parts of the
236 marine platform, GA22-13 from the foresets and GA22-14 from the topset, suggesting they best
237 represent the age of the feature itself. One of the ages, GA22-12, is >109 ka, and may not have
238 been fully bleached at the time of deposition or may indicate a composite landform of more than
239 one age (e.g. Malatesta et al., 2022). The fourth age, GA22-15, is younger than the first two at
240 24 ka. Its younger age may suggest reworking of the deposits during the LGM. The diamicton,
241 likely glacial in origin, is found at the base of the pre-LGM marine deposits making this till
242 demonstrably pre-LGM in age, possibly MIS 4.

243 If the high marine terrace at Slaggan Bay pre-dates the LGM, how did it survive being
244 overridden by an ice sheet? Pre-MIS 2 sedimentary deposits are known to have survived the last
245 glaciation in a number of locations across Scotland (Merritt et al., 2019). These deposits are
246 widespread in parts of NE Scotland where the extent and depth of glacial erosion was limited,
247 but are relatively rare along Scotland's western seaboard. Bradwell (2013) mapped zones of past
248 ice streaming around Loch Laxford ca. 60 km to the north of Slaggan Bay. He used the extent
249 and degree of glacial erosional forms and the preservation of mountain-top pre-glacial debris to
250 map zones of former fast-flowing ice and infer former areas of warm- and cold-based ice.
251 Bradwell (2013) found that regions of intense glacial erosion were spatially interspersed with
252 regions of very little glacial modification or preservation, which he interpreted as cold-based
253 'frozen-bed patches'. It is plausible that the western part of the Greenstone Peninsula was
254 located in a slow-flowing or frozen-bed patch between zones of streaming ice on either side. The
255 deep bathymetry of Loch Ewe and around the Summer Isles (outer Loch Broom) would have
256 promoted ice-flow funneling and enhanced basal melting. The large glaciers flowing along these
257 troughs would have fed into the Minch paleo-ice stream at times of maximum glaciation, leaving
258 the higher ground and lee-side slopes of the Greenstone Point and Stoer peninsulas in regions of
259 relatively low erosion. Numerical ice-sheet modelling by Hubbard et al. (2009) supports this idea
260 with slow flowing (cold-based) zones existing on these headlands at various times during the last
261 40,000 years.

262 *5.2 MIS 3 sea levels across Scotland*

263 We interpret the two congruent ages (53.5 and 49.4 ka) to represent the age of the high
264 marine terrace at Slaggan Bay. Thus, the marine terrace at Slaggan Bay provides a constraint on
265 MIS 3 sea levels for Scotland. The elevation of the top of the platform is 28 m OD. This

266 elevation is 8-9 m higher than the post-LGM marine limit of 19.3 m on Greenstone Point with
267 shorelines reaching as high as 20.4 m at the northeastern edge of the peninsula in Gruinard Bay
268 (Fig. 1; Sissons and Dawson, 1981).

269 Although not dated but similar to the case at Slaggan Bay, the surveyed elevations of the
270 25 m marine terrace at Stoer Peninsula are much higher than the ~6 m post-LGM marine limit at
271 this location (Hamilton et al., 2015). Other undated hypothesized pre-LGM beaches are found at
272 elevations higher than the post-LGM marine limit to the south of Slaggan Bay on the Applecross
273 Peninsula (Robinson, 1977). Dated MIS 3 marine deposits and shorelines higher than the post-
274 LGM marine limit have also been found on the Island of Islay (Dawson et al., 1997) farther
275 south in Scotland and in southern Ireland (O’Cofaigh et al., 2012; Gallagher et al., 2015)
276 suggesting fragments of these higher shorelines are not isolated to Slaggan Bay or Stoer
277 Peninsula. What conditions would be required to produce MIS 3 RSLs higher than MIS 2
278 Lateglacial shorelines across NW Scotland?

279 *5.3 Potential implications for the glacial history of NW Scotland*

280 We compared our new MIS 3 sea-level constraints to GIA model predictions using the
281 GLAC1D+ ice reconstruction, which contains no ice over Scotland during MIS 4, and the
282 PALEOMIST ice sheet reconstruction, which contains significantly more ice over the northern
283 Hemisphere including Scotland during MIS 4. The MIS 3 RSL predictions for NW Scotland
284 differ significantly between these two models but are very similar for the LGM and post-LGM
285 period (Fig. 4). Assuming the Slaggan Bay marine terrace formed during the period of highest
286 MIS 3 RSLs in Scotland (at 57.5 ka according to the PALEOMIST model, 56 ka in the
287 GLAC1D+ model, both within error of the average of the two OSL ages of 51.5 ± 6.7 ka), the
288 GLAC1D+ model predicts RSLs at Slaggan Bay of about -48 m, nearly 70 m lower than the

289 observed MIS 3 RSLs. The PALEOMIST predictions for Slaggan Bay are much higher,
290 reaching elevations as high as +12.7 m around 57 ka. Although a 15 m difference remains
291 between our new observed MIS 3 RSLs and the predictions using the PALEOMIST
292 reconstruction, the fit is nearly 55 m better than the GLAC1D+ reconstruction. This
293 improvement is not simply a function of higher GMSLs within the PALEOMIST reconstruction,
294 as at the time of the Scottish MIS 3 highstand, GMSL is lower than that of the GLAC1D+ model
295 (Fig. 4). The better fit is due to the postglacial rebound caused by retreat of the MIS 4 ice sheet
296 over Scotland (Fig. 4). In addition, the timing of the MIS 3 highstand in Scotland is notable
297 within the GIA predictions. For the PALEOMIST prediction, the highest GMSLs occur at 42.5
298 ka, while the local Scottish MIS 3 highstand occurs at 57 ka, which agrees with our new OSL
299 ages. Thus, the simplest way to reconcile the 28 m MIS 3 RSLs at Slaggan Bay with the lower-
300 than-present GMSLs during MIS 3 is for an ice sheet to have existed over Scotland during MIS 4
301 and melted during early MIS 3. The size of the ice sheet needs refinement, as bringing the
302 PALEOMIST predictions into agreement with our new RSL data requires a slightly larger ice
303 mass than that of PALEOMIST. This observation contributes to the growing body of evidence
304 for a significant ice sheet on the British Isles during MIS 4 (e.g. Siegert et al., 2001; Hibbert et
305 al., 2010; Gallagher et al., 2015; Hughes et al., 2022; Scourse, 2024) and for GMSLs during MIS
306 3 to be higher than predicted from oxygen isotope records alone (e.g. Dalton et al., 2022a).

307 In their current form, the GIA model predictions for ice-sheet models containing ice over
308 Scotland during MIS 4 cannot explain all discrepancies in MIS 3 RSL histories across NW
309 Scotland and the British Isles. For example, the PALEOMIST model does not contain ice over
310 Ireland during MIS 4, which without ice does not produce the isostatic rebound needed to
311 generate the higher than present sea levels across southern Ireland observed at Courtmacsherry

312 by O’Cofaigh et al. (2012)(e.g. Fig. S1). Similarly, although the observed differences in the
313 elevations of the pre-LGM shorelines at Slaggan Bay and Stoer are on the order of 3 m, the
314 difference between the PALEOMIST predictions of MIS 3 RSLs are closer to 13 m (e.g. Fig.
315 S1). However, the Stoer shoreline remains undated and thus may not correlate to the same RSL
316 highstand as Slaggan Bay. Alternatively, the ice sheet may have had a different configuration
317 during MIS 4 than the ice sheet reconstruction of the PALEOMIST model. Another possibility
318 for the larger difference in elevations of the post-glacial shorelines compared to the pre-LGM
319 shorelines is that the post-glacial marine limits are underestimated near Stoer (Puckette et al.,
320 2024).

321 **Conclusions**

322 We provide new OSL ages from a marine terrace 8-9 m higher than the post-LGM
323 marine limit near Greenstone Point, NW Scotland. The ages suggest the feature dates to MIS 3
324 providing one of the few dated constraints on sea levels at this time for Scotland. Other similar
325 higher-than expected marine features of unknown age are found in NW Scotland and some dated
326 MIS 3 shorelines and marine deposits are found in other areas within the British Isles, suggesting
327 these fragments are not isolated to Slaggan Bay. As global sea levels are thought to be 40-60 m
328 lower than present during this time, the elevation of the marine terrace at 28 m requires a
329 significant GIA contribution. Glacial isostatic adjustment model predictions suggest a
330 significant ice mass over Scotland during MIS 4 could explain the anomalously high MIS 3
331 relative sea levels for this part of Scotland. Our work adds to a growing body of research
332 suggesting pre-LGM features can be preserved beneath an ice sheet in the right subglacial
333 conditions and that a significant MIS 4 ice sheet grew over Scotland.

334

335 **Acknowledgements**

336 We thank Elisa Medri, Claire Divola, Jennifer Taylor, and Lauren Mumby for their
337 assistance in the field. This work was supported by NSFGE0-NERC Grants #2147750 and
338 #2147752. SLB, LB, TB and JL were funded by UK Natural Environmental Research Council
339 (NERC) grant numbers NE/X009459/1, NE/X009343/1, NE/X009378/1 and NE/X009335/1
340 respectively. The authors would like to thank the insightful reviews of Fiona Hibbert and two
341 anonymous reviewers. This work benefited from discussions with the broader PALSEA
342 community.

343 **References:**

- 344 Batchelor, C.L., Margold, M., Krapp, M., Murton, D.K., Dalton, A.S., Gibbard, P.L., Stokes,
345 C.R., Murton, J.B., & Manica, A. (2019). The configuration of Northern Hemisphere ice
346 sheets through the Quaternary. *Nature Communications*, 10, 3713.
- 347 Bowen, D.Q. (1991). Time and space in the glacial sediment systems of the British Isles. In:
348 Ehlers, J., Gibbard, P.L., & Rose, J. (Eds.). *Glacial Deposits in Great Britain and Ireland*.
349 Rotterdam, Balkema, 3-11.
- 350 Bowen, D.Q., Phillips, F.M., McCabe, A.M., Knutz, P.C., & Sykes, G.A. (2002). New data for
351 the Last Glacial Maximum in Great Britain and Ireland. *Quaternary Science Reviews*,
352 21, 89-101.
- 353 Bradley, S. L., Ely, J. C., Clark, C. D., Edwards, R. J., & Shennan, I. (2023). Reconstruction of
354 the palaeo-sea level of Britain and Ireland arising from empirical constraints of ice
355 extent: implications for regional sea level forecasts and North American ice sheet
356 volume. *Journal of Quaternary Science*, 38, 791–805.
- 357 Bradwell, T. (2013). Identifying palaeo-ice-stream tributaries on hard beds: Mapping glacial

358 bedforms and erosion zones in NW Scotland. *Geomorphology*, 201, 397-414.

359 Bradwell, T., Fabel, D., Clark, C. D., Chiverrell, R. C., Small, D., Smedley, R. K., et al. (2021).

360 Pattern, style, and timing of British-Irish Ice Sheet advance and retreat over the last 45

361 000 years: evidence from NW Scotland and the adjacent continental shelf. *Journal of*

362 *Quaternary Science*, 36, 871–933.

363 Clark, C. D., Gibbard, P. L., & Rose, J. (2004). Pleistocene glacial limits in England, Scotland,

364 and Wales. In J. Ehlers & P. L. Gibbard (Eds.), *Quaternary Glaciations - Extent and*

365 *Chronology* (Vol. 2, pp. 47–82). Elsevier.

366 Clark, C. D., Ely, J. C., Greenwood, S. L., Hughes, A. L. C., Meehan, R., Barr, I. D., et al.

367 (2018). BRITICE Glacial Map, version 2: a map and GIS database of glacial landforms

368 of the last British-Irish Ice Sheet. *Boreas*, 47, 11-e8.

369 Dalton, A. S., Finkelstein, S. A., Forman, S. L., Barnett, P. J., Pico, T., & Mitrovica, J. X.

370 (2019). Was the Laurentide Ice Sheet significantly reduced during Marine Isotope Stage

371 3? *Geology*, 47, 111–114.

372 Dalton, A. S., Stokes, C. R., & Batchelor, C. L. (2022). Evolution of the Laurentide and Innuitian

373 ice sheets prior to the Last Glacial Maximum (115 ka to 25 ka). *Earth-Science Reviews*,

374 224, 103875.

375 Dalton, A. S., Pico, T., Gowan, E. J., Clague, J. J., Forman, S. L., McMartin, I., et al. (2022). The

376 marine $\delta^{18}O$ record overestimates continental ice volume during Marine Isotope Stage

377 3. *Global and Planetary Change*, 212, 103814.

378 Dawson, A.G., Benn, D.I., & Dawson, S. (1997). Late Quaternary glaciomarine sedimentation

379 in the Rhinns of Islay, Scottish Inner Hebrides. In: Dawson, A.G. & Dawson, S. (eds.):

380 The Quaternary of Islay and Jura: Field Guide. Quaternary Research Association. p. 66-

381 77.

382 Dawson, A.G., Best, L., & Simms, A.R. (2023). Raised shorelines and late Quaternary relative
383 sea-level changes in Wester Ross. In: Ballantyne, C.K. (ed.). *The Quaternary of Wester*
384 Ross: Field Guide. Quaternary Research Association. p. 163-180.

385 Dawson, A. G., Bishop, P., Hansom, J., & Fabel, D. (2022). ^{10}Be exposure age dating of Late
386 Quaternary relative sea level changes and deglaciation of W Jura and NW Islay, Scottish
387 Inner Hebrides. *Earth and Environmental Science Transactions of the Royal Society of*
388 *Edinburgh*, 113, 253–266.

389 Doughty, A.M., Kaplan, M.R., Peltier, C., & Barker, S. (2021). A maximum in global glacier
390 extent during MIS 4. *Quaternary Science Reviews*, 261, 106948.

391 Duller, G.A.T. (2003). Distinguishing quartz and feldspar in single grain luminescence
392 measurements. *Radiation Measurements*, 37, 161–165.

393 Duller, G.A.T., Wintle, A.G., & Hall, A.M. (1995). Luminescence dating and its application to
394 key pre-late Devensian sites in Scotland. *Quaternary Science Reviews*, 14, 495-519.

395 Fabian, S.G., Gallacher, S.J., & De Vleeschouwer, D. (2023). British–Irish Ice Sheet and polar
396 front history of the Goban Spur, offshore southwest Ireland over the last 250 000 years.
397 *Boreas*, 52, 476-497.

398 Finlayson, A., Merritt, J., Browne, M., Merritt, J., & McMillan, A. (2010). Ice sheet advance,
399 dynamics, and decay configurations: evidence from west central Scotland. *Quaternary*
400 *Science Reviews*, 29, 969–988.

401 Galbraith, R.F., Roberts, R.G., Laslet, G.M., Yoshida, H., & Olley, J.M. (1999). Optical dating
402 of single and multiple grains of quartz from Jinmium rock shelter, northern Australia:
403 Part I, Experimental design and statistical models. *Archaeometry*, 41, 339–364.

404 Gallagher, C., Telfer, M. W., & O Cofaigh, C. (2015). A Marine Isotope Stage 4 age for
405 Pleistocene raised beach deposits near Fethard, southern Ireland. *Journal of Quaternary*
406 *Science*, *30*, 754–763.

407 Gemmell, A. M. D., Murray, A. S., & Connell, E. R. (2007). Devensian glacial events in Buchan
408 (NE Scotland): A progress report on new OSL dates and their implications. *Quaternary*
409 *Geochronology*, *2*, 237–242.

410 Gibbard, P. L., & Clark, C. D. (2011). Chapter 7: Pleistocene glaciation limits in Great Britain.
411 *Developments in Quaternary Science*, *15*, 75–93.

412 Gowan, E. J., Zhang, X., Khosravi, S., Rovere, A., Stocchi, P., Hughes, A. L. C., et al. (2021). A
413 new global ice sheet reconstruction for the past 80 000 years. *Nature Communications*,
414 *12*, 1199. [A new global ice sheet reconstruction for the past 80 000 years | Nature](#)
415 [Communications](#))

416 Hamilton, C. A., Lloyd, J. M., Barlow, N. L. M., Innes, J. B., Flecker, R., & Thomas, C. P.
417 (2015). Late glacial to Holocene relative sea-level change in Assynt, northwest Scotland,
418 UK. *Quaternary Research*, *84*, 214–222.

419 Hibbert, F. D., Austin, W. E. N., Leng, M. J., & Gatliff, R. W. (2010). British Ice Sheet
420 dynamics inferred from North Atlantic ice-rafted debris records spanning the last 175 000
421 years. *Journal of Quaternary Science*, *25*, 461–482.

422 Hubbard, A., Bradwell, T., Golledge, N., Hall, A., Patton, H., Sugden, D., Cooper, R., & Stoker,
423 M. (2009). Dynamic cycles, ice streams and their impact on the extent, chronology and
424 deglaciation of the British-Irish ice sheet. *Quaternary Science Reviews*, *28*, 758-776.

425 Hughes, A. L. C., Gyllencreutz, R., Lohne, O. S., Mangerud, J., & Svendsen, J. I. (2016). The
426 last Eurasian ice sheets - a chronological database and time-slice reconstruction,

427 DATED-1. *Boreas*, 45, 1–45.

428 Hughes, P. D., Glasser, N. F., & Fink, D. (2022). ¹⁰Be and ²⁶Al exposure history of the highest
429 mountains in Wales: Evidence from Yr Wyddfa (Snowdon) and Y Glyderau for a
430 nunatak landscape at the global Last Glacial Maximum. *Quaternary Science Reviews*,
431 286, 107523.

432 Kendall, R. A., Mitrovica, J. X. & Milne, G. A. (2005), On post-glacial sea level – II. Numerical
433 formulation and comparative results on spherically symmetric models. *Geophysical*
434 *Journal International*, 161, 679–706.

435 Kleman, J., Hattestrand, M., Borgstrom, I., Fabel, D., & Preusser, F. (2021). Age and duration of
436 a MIS 3 interstadial in the Fennoscandian Ice Sheet core area - implications for ice sheet
437 dynamics. *Quaternary Science Reviews*, 264, 107011.

438 Knutz, P.C., Austin, W.E.N., & Jones, E.J.W. (2001). Millennial-scale depositional cycles
439 related to British Ice Sheet variability and North Atlantic paleocirculation since 45 kyr
440 B.P., Barra Fan, U.K. margin. *Paleoceanography*, 16, 53-64.

441 Malatesta, L. C., Finnegan, N. J., Huppert, K. L., & Carreno, E. I. (2022). The influence of rock
442 uplift rate on the formation and preservation of individual marine terraces during multiple
443 sea-level stands. *Geology*, 50, 101–105.

444 Merritt, J. W., & Auton, C. A. (2000). An outline of the lithostratigraphy and depositional
445 history of Quaternary deposits in the Sellafield district, west Cumbria. *Proceedings of the*
446 *Yorkshire Geological Society*, 53, 129–154.

447 Merritt, J. W., Hall, A. M., Gordon, J. E., & Connell, E. R. (2019). Late Pleistocene sediments,
448 landforms and events in Scotland: A review of the terrestrial stratigraphic record. *Earth*
449 *and Environmental Science Transactions of the Royal Society of Edinburgh*, 110, 39–91.

450 Mitrovica, J. X. & Milne, G. A. (2003), On post-glacial sea level: I. General theory. *Geophysical*
451 *Journal International*, 154, 253–267.

452 O’Cofaigh., C., Telfer, M.W., Bailey, R.M., & Evans, D.J.A. (2012). Late Pleistocene
453 chronostratigraphy and ice sheet limits, southern Ireland. *Quaternary Science Reviews*,
454 44, 160-179.

455 Peck, V.L., Hall, I.R., Zahn, R., Grousset, F., Hemming, S.R., & Scourse, J.D. (2007). The
456 relationship of Heinrich events and their European precursors over the past 60 ka BP: a
457 multi-proxy ice-rafted debris provenance study in the North East Atlantic. *Quaternary*
458 *Science Reviews*, 26, 862-875.

459 Peltier, C., Kaplan, M.R., Birkel, S.D., Soteres, R.L., Sagredo, E.A., Aravena, J.C., Araos, J.,
460 Moreno, P.I., Schwartz, R., & Schaefer, J.M. (2021). The large MIS 4 and long MIS 2
461 glacier maxima on the southern tip of South America. *Quaternary Science Reviews*, 262,
462 106858.

463 Pico, T., Birch, L., Weisenberg, J., & Mitrovica, J. X. (2018). Refining the Laurentide Ice Sheet
464 at Marine Isotope Stage 3: A data-based approach combining glacial isostatic simulations
465 with a dynamic ice model. *Quaternary Science Reviews*, 195, 171–179.

466 Pico, T., McGee, D., Russell, J., & Mitrovica, J. X. (2020). Recent constraints on MIS 3 sea level
467 support role of continental shelf exposure as a control on Indo-Pacific hydroclimate.
468 *Paleoceanography and Paleoclimatology*, 32, e2020PA003998.

469 Prescott, J.R. & Hutton, J.T. (1994). Cosmic ray contributions to dose rates for luminescence and
470 ESR dating: Large depths and long-term time variations. *Radiation Measurements*, 23,
471 497–500.

472 Puckette, T.P., Simms, A.R., Best, L., Lloyd, J.M., Bradwell, T., & Small, D. (2024). New

473 constraints on post-glacial relative sea-level changes from isolation basins across NW
474 Scotland. Geological Society of America Abstracts with Program, 56, 2024. doi:
475 10.1130/abs/2024AM-402812.

476 Rex, C.L., Bateman, M.D., Buckland, P.C., Panagiotakopulu, E., Livingstone, S.J., Hardiman,
477 M., & Eddey, L. (2023). A revision of the British chronostratigraphy within the last
478 glacial-interglacial cycle based on new evidence from Arclid, Cheshire UK. *Quaternary*
479 *Science Reviews*, 299, 107882.

480 Robinson, M. (1977). *Glacial Limits, Sea-Level Changes and Vegetation Development in Part of*
481 *Wester Ross*. University of Edinburgh.

482 Robinson, M. & Ballantyne, C.K. (1979). Evidence for a glacial readvance pre-dating the Loch
483 Lomond advance in Wester Ross. *Scottish Journal of Geology*, 15, 271-277.

484 Rolfe, C.J., Hughes, P.D., Fenton, C.R., Schnabel, C., Xu, S. & Brown, A.G. (2012). Paired
485 ²⁶Al and ¹⁰Be exposure ages from Lundy: new evidence for the extent and timing of
486 Devensian glaciation in the southern British Isles. *Quaternary Science Reviews*, 43, 61-
487 73.

488 Scourse, J. D. (2024). The timing and magnitude of the British-Irish Ice Sheet between Marine
489 Isotope Stages 5d and 2: implications for glacio-isostatic adjustment, high relative sea
490 levels and “giant erratic” emplacement. *Journal of Quaternary Science*, 39, 505–514.

491 Scourse, J.D., Haapaniemi, A.I., Colmenero-Hidalgo, E., Peck, V.L., Hall, I.R., Austin, W.E.N.,
492 Knutz, P.C., & Rainer, Z. (2009). Growth, dynamics, and deglaciation of the last
493 British-Irish ice sheet: the deep-sea ice-rafted detritus record. *Quaternary Science*
494 *Reviews*, 28, 3066-3084.

495 Shennan, I., Bradley, S.L., & Edwards, R. (2018). Relative sea-level changes and crustal

496 movements in Britain and Ireland since the Last Glacial Maximum. *Quaternary Science*
497 *Reviews*, 188, 143-159.

498 Siddall, M., Rohling, E. J., Thompson, W. G., & Waelbroeck, C. (2008). Marine Isotope Stage 3
499 sea level fluctuations: data synthesis and new outlook. *Reviews of Geophysics*, 46, 1-29
500 (2007RG000226).

501 Simms, A.R., Best, L., Shennan, I., Bradley, S.L., Small, D., Bustamante, E., Lightowler, A.,
502 Osleger, D., & Sefton, J. (2022). Investigating the roles of relative sea-level change and
503 glacio-isostatic adjustment on the retreat of a marine based ice stream in NW Scotland.
504 *Quaternary Science Reviews*, 277, 107366.

505 Siebert, M. J., Dowdeswell, J. A., Hald, M., & Svendsen, J. I. (2001). Modelling the Eurasian Ice
506 Sheet through a full (Weichselian) glacial cycle. *Global and Planetary Change*, 31, 367–
507 385.

508 Sissons, J. B., & Dawson, A. G. (1981). Former sea-levels and ice limits in part of Wester Ross,
509 northwest Scotland. *Proceedings of the Geologists' Association*, 92, 115–124.

510 Smith, D. E., Fretwell, P. T., Cullingford, R. A., & Firth, C. R. (2006). Towards improved
511 empirical isobase models of Holocene land uplift for mainland Scotland, UK.
512 *Philosophical Transactions of the Royal Society A*, 364, 949–972.

513 Smith, D. E., Barlow, N. L. M., Bradley, S. L., Firth, C. R., Hall, A. M., Jordan, J. T., & Long,
514 D. (2019). Quaternary sea level change in Scotland. *Earth and Environmental Science*
515 *Transactions of the Royal Society of Edinburgh*, 110, 219–256.

516 Sutherland, D.G. (1981). The high-level marine shell beds of Scotland and the build-up of the
517 last Scottish ice sheet. *Boreas*, 10, 247-254.

518 Tarasov, L., Dyke, A. S., Neal, R. M., & Peltier, W. R. (2012). A data-calibrated distribution of

519 deglaical chronologies for the North American ice complex from glaciological modeling.
520 *Earth and Planetary Science Letters*, 315–316, 30–40.

521 Thierens, M., Pirlet, H., Colin, C., Latruwe, K., Vanhaecke, F., Lee, J. R., et al. (2012). Ice-
522 rafting from the British-Irish ice sheet since the earliest Pleistocene (2.6 million years
523 ago): implications for long-term mid-latitude ice-sheet growth in the North Atlantic
524 region. *Quaternary Science Reviews*, 44, 229–240.

525 Toucanne, S., Zaragosi, S., Bourillet, J.F., Gibbard, P.I., Eynaud, F., Giraudeau, J., Turon, J.L.,
526 Cremer, M., Corgiho, E., Martinez, P., & Rossignol, L. (2009). A 1.2 Ma record of
527 glaciation and fluvial discharge from the West European Atlantic margin. *Quaternary
528 Science Reviews*, 28, 2974-2981.

529 Toucanne, S., Rodrigues, T., Menot, G., Soulet, G., Cheron, S., Billy, I., et al. (2023). Marine
530 Isotope Stage 4 (71-57 ka) on the Western European margin: Insights to the drainage and
531 dynamics of the Western European Ice Sheet. *Global and Planetary Change*, 229,
532 104221.

533 Wilson, L.J., Austin, W.E.N., & Jansen, E. (2002). The last British Ice Sheet: Growth,
534 maximum extent and deglaciation. *Polar Research*, 21, 243-250.

535 Wintle, A. G., & Murray, A. S. (2006). A review of quartz optically stimulated luminescence
536 characteristics and their relevance in single-aliquot regeneration dating protocols.
537 *Radiation Measurements*, 41, 369–391.

538 Yokoyama, Y., Lambeck, K., De Deckker, P., Esat, T.M., Webster, J.M., & Nakada, M. (2021).
539 Towards solving the missing ice problem and the importance of rigorous model data
540 comparisons. *Nature Communications*, 13, 6261.

541

542 **Tables**

543 Table 1. Dose results for the OSL samples

544 Table 2. Dose rate information for the OSL samples.

545

546 **Figure Legends:**

547 Figure 1. Map of the British Isles showing the general location of our study area (a). Hillshade
548 model of northwest Scotland (b) and satellite image of Gairloch and Greenstone Point
549 Peninsulas (c) and Slaggan Bay (d) (from GoogleEarth) illustrating the locations of
550 places mentioned in the text. Stars in (a) are the locations of previously reported
551 potential MIS 3/4 sites including Courtmacsherry (1, O' Cofaigh et al., 2012), Fethard (2,
552 Gallagher and Thorpe, 1997; O' Cofaigh et al., 2012), Isle of Islay (3, Dawson et al.,
553 1997), Suainebost (4, Bradwell et al., 2021), Alt Odhar (5) and Howe of Byth (6)(Duller
554 et al., 1995), Aberdeen (7, Gemmell et al., 2007), Arclid Quarry (8, Rex et al., 2023),
555 Snowdon (9, Hughes et al., 2022), and Lundy Island (10, Rolfe et al., 2012). Blue stars
556 in (a) represent outwash deposits while yellow stars represent beach deposits and red
557 stars represent glacial landforms or till. Ire. = Ireland, GB = Great Britain. White
558 triangles in (c) are the altitudes (in meters) of lateglacial shoreline features mapped by
559 Sissons and Dawson (1981), while the dashed line represents the extent of a post-LGM
560 ice sheet readvance known as the Wester Ross Readvance (from Robinson and
561 Ballantyne, 1979).

562 Figure 2. Photographs of the marine terraces and their cover deposits at Slaggan Bay (a, b, d, e,
563 f) and Stoer Peninsula (c, g). (a) Photograph looking south and up at the marine terrace
564 from near the coastline below sample GA22-14 (see Figure 1). Also shown is the
565 locations of the other OSL samples and the unconformity between the Torridonian

566 Sandstone below and Quaternary deposits above. (b) Photograph taken from the top of
567 the marine terrace at Slaggan Bay looking north at the location of OSL sample GA22-14.
568 (c) The marine terrace at Stoer. (d) The well-cemented gravelly sand and sandy gravels
569 comprising the “topsets” of the marine platform at Slaggan Bay at the location of OSL
570 sample GA22-14, (e), The interbedded sands and silts of the “forsets” of the marine
571 platform at Slaggan Bay. (f) The till at the base of the Quaternary section at Slaggan
572 Bay. (g) The till underlying and cut by the wave-cut platform at Stoer.

573 Figure 3. Cartoon summarizing the sedimentary deposits and geomorphology at Slaggan Bay.

574 Figure 4. (a) Model predictions of past GMSL (dashed lines) and RSL (solid lines) for two
575 different GIA models, PALEOMIST (Gowan et al., 2021; red) and GLAC1D+ (Bradley
576 et al., 2023; black). Also shown are the age and elevation of the marine platform-based
577 RSL observations from Slaggan Bay (grey boxes) as well as the periods of ice cover
578 within the two GIA models, PALEOMIST (Gowan et al., 2021, blue box) and GLAC1D+
579 (Bradley et al., 2023; hashed box).

580

581 Supporting Information

582 Fig. S1. PALEOMIST predictions or RSL for Stoer, Slaggan Bay, and Courtmacsherry.

583

584

585

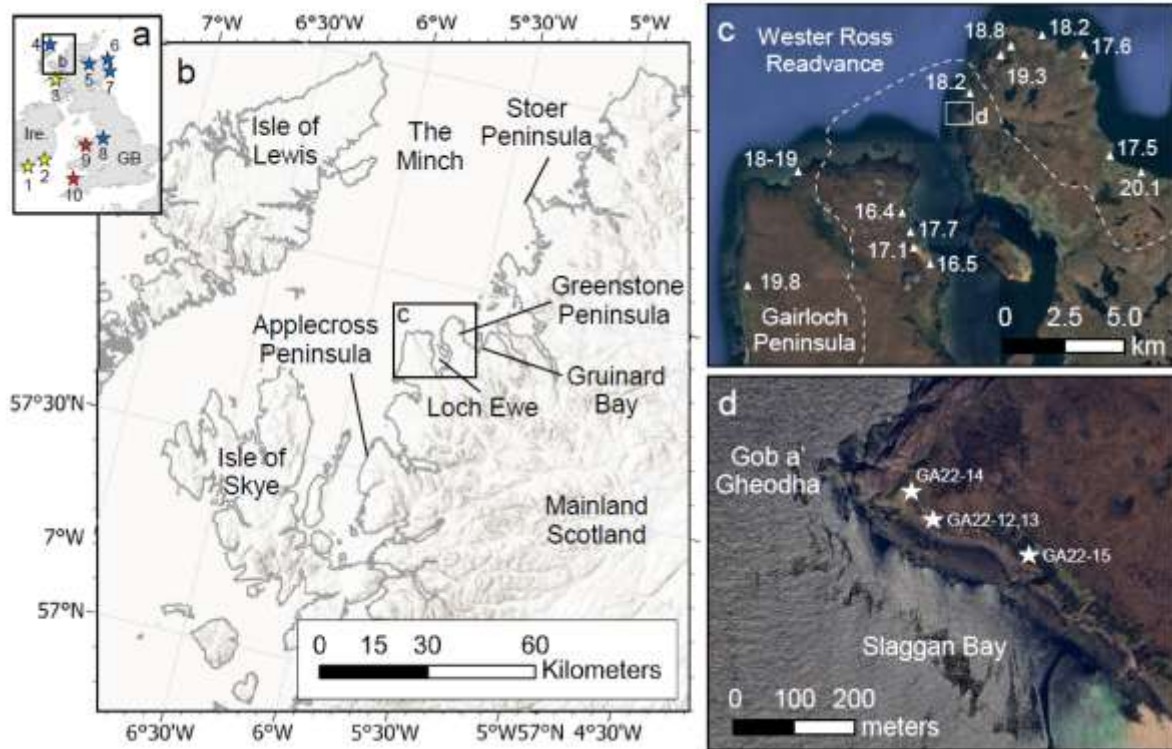
586

587

588

589

590 Figure 1.

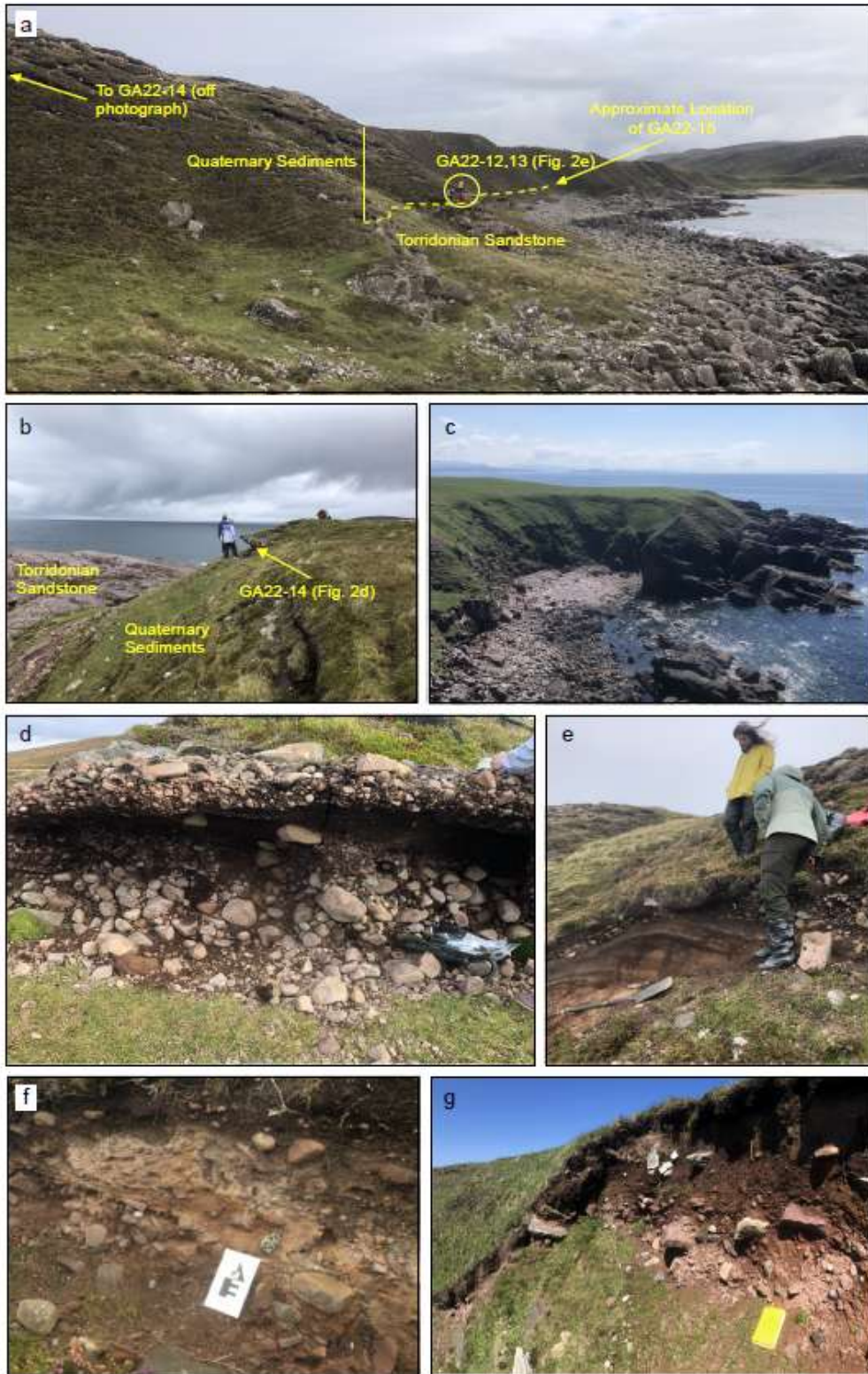


591

592

593

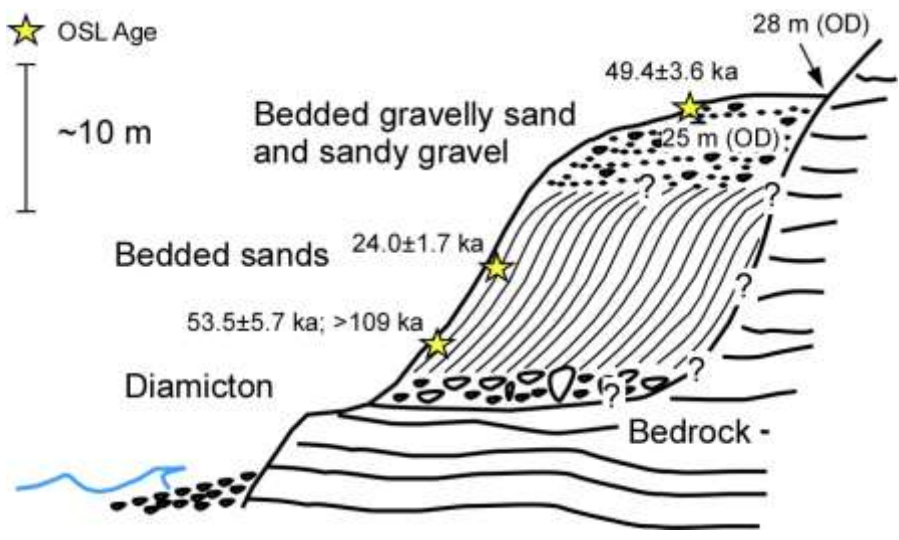
594 Figure 2.



595

596

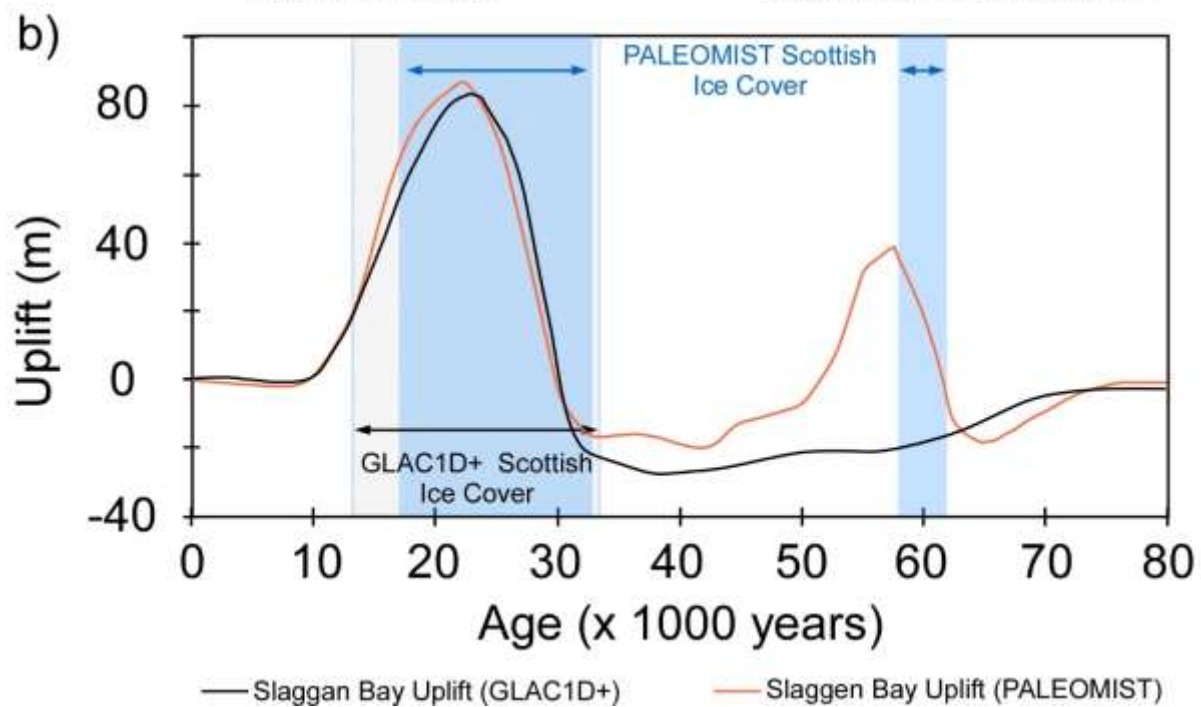
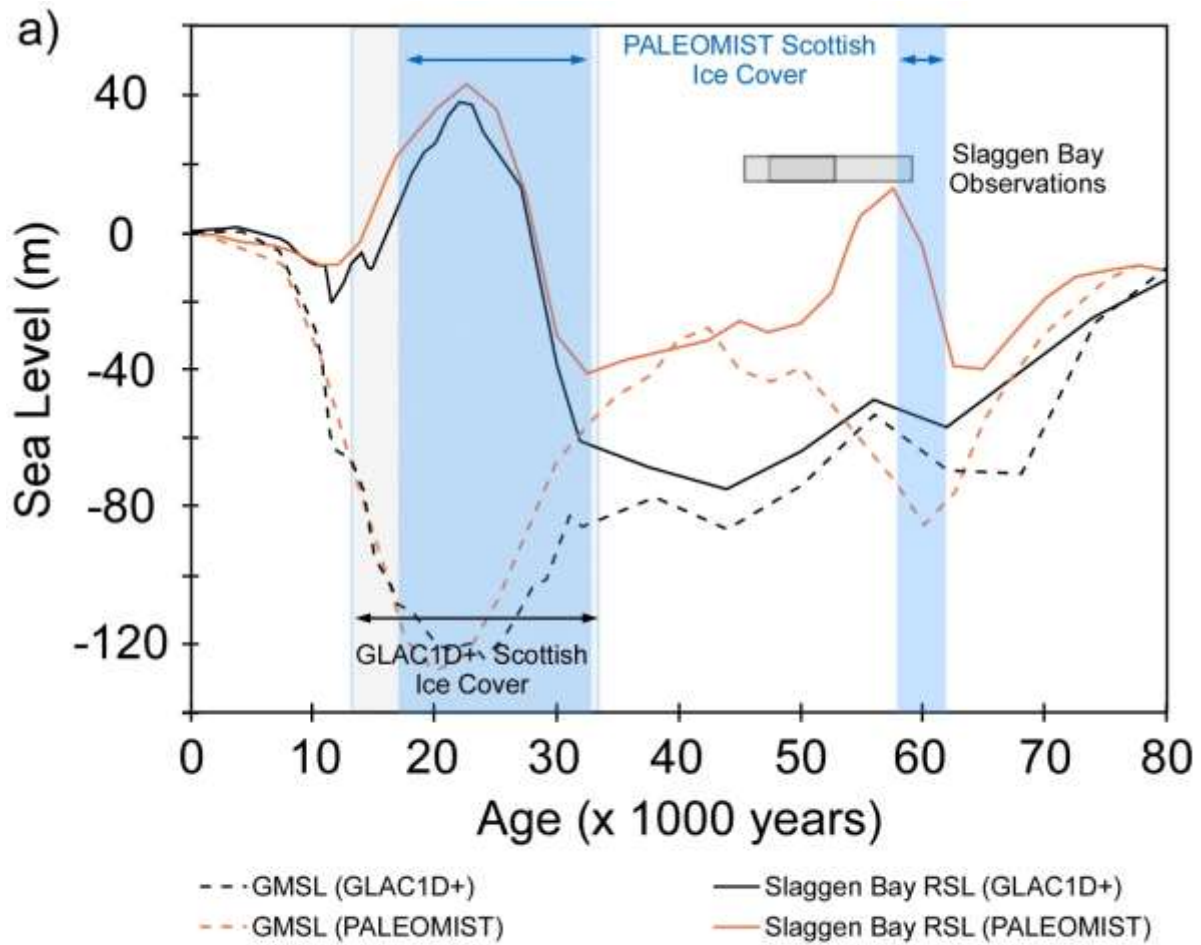
597 Figure 3.



598

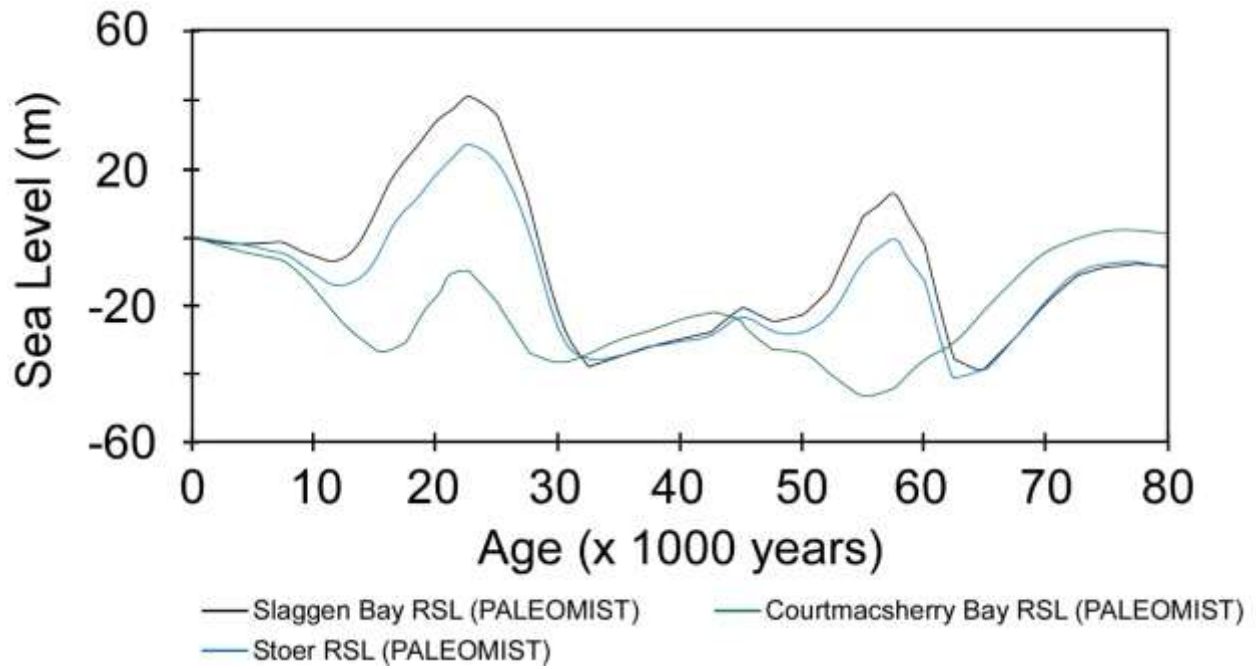
599

600 Figure 4.



601

602 Figure S1.



603

604

605

606

607

608 Table 1.

609

Sample	grain size (μm)	n [†] measured	n [†] used	Dose (Gy) [‡]	overdispersion (%)
GA22-12	150-180	11	11	302.8 \pm 22.95 [§]	N/A
GA22-13	150-180	29	28	139.1 \pm 8.9	18
GA22-14	180-212	41	35	132.9 \pm 8.5	20
GA22-15	90-125	30	25	53.3 \pm 3.3	12

[†]number of aliquots

[‡]1-sigma uncertainty

610 [§]Sample GA22-12 was in saturation and the dose reflects the saturation dose of 2D₀

611

612 Table 2.

Sample	Th (ppm)	U (ppm) ² from Th234	U (ppm) from Bi214	K (%)	water factor	DR beta (Gy/ka)	DR Gamma (Gy/ka)	DR cosm (Gy/ka)	DR total (Gy/ka)
GA22-12 ⁵						1.881 ± 0.090	0.798 ± 0.029	0.0957 ± 0.0048	2.774 ± 0.094
GA22-13 ⁵						1.763 ± 0.221	0.758 ± 0.035	0.0811 ± 0.0041	2.602 ± 0.224
GA22-12/13 g1	3.81 ± 0.35	1.73 ± 0.36	0.800 ± 0.049	2.33 ± 0.11	0.06 ± 0.01				
GA22-12/13 g2	4.96 ± 0.37	1.61 ± 0.34	1.057 ± 0.059	2.42 ± 0.12	0.15 ± 0.03				
GA22-12/13 ⁴ g3	3.82 ± 0.29	1.78 ± 0.31	0.842 ± 0.055	2.14 ± 0.10	0.05 ± 0.01				
GA22-12/13 g4	3.22 ± 0.28	1.94 ± 0.33	0.711 ± 0.048	2.05 ± 0.10	0.08 ± 0.01				
GA22-14						1.747 ± 0.088	0.739 ± 0.027	0.2045 ± 0.0102	2.690 ± 0.092
GA22-14 g1 ¹	3.51 ± 0.27	2.15 ± 0.33	0.695 ± 0.044	2.10 ± 0.10	0.05 ± 0.01				
GA22-14 g2	4.87 ± 0.47	1.52 ± 0.40	0.959 ± 0.068	2.31 ± 0.11	0.02 ± 0.01				
GA22-15						1.465 ± 0.080	0.681 ± 0.015	0.0694 ± 0.0035	2.216 ± 0.082
GA22-15 g1	3.65 ± 0.33	0.72 ± 0.19	0.650 ± 0.048	1.75 ± 0.09	0.08 ± 0.01				
GA22-15 g2 ¹	4.79 ± 0.41	0.56 ± 0.13	0.857 ± 0.057	1.94 ± 0.09	0.15 ± 0.03				
GA22-15 g3	4.46 ± 0.38	1.18 ± 0.21	1.212 ± 0.078	1.77 ± 0.09	0.00 ± 0.01				

Nuclide concentrations and water contents are listed for each of the separate layers. ¹The layer from which the OSL sample was collected.

²Uranium concentrations obtained from the 92keV emission of Th234 as well as the concentrations obtained from the emissions of Bi214 and Pb214.

⁵Samples GA22-12 and GA22-13 were taken from the same site, but different layers.

613